Chapter 9
Structure of the MCM2-7 Double Hexamer and Its Implications for the Mechanistic Functions of the Mcm2-7 Complex

Yuanliang Zhai and Bik-Kwoon Tye

Abstract The eukaryotic minichromosome maintenance 2–7 complex is the core of the inactive MCM replication licensing complex and the catalytic core of the Cdc45-MCM-GINS replicative helicase. The years of effort to determine the structure of parts or the whole of the heterohexameric complex by X-ray crystallography and conventional cryo-EM produced limited success. Modern cryo-EM technology ushered in a new era of structural biology that allowed the determination of the structure of the inactive double hexamer at an unprecedented resolution of 3.8 Å. This review will focus on the fine details observed in the Mcm2-7 double hexameric complex and their implications for the function of the Mcm2-7 hexamer in its different roles during DNA replication.

Keywords DNA replication • Replication licensing • MCM2-7 • Cryo-EM structure

Y. Zhai
Division of Life Science, Hong Kong University of Science and Technology, Hong Kong, China

Institute for Advanced Study, Hong Kong University of Science and Technology, Hong Kong, China

B.-K. Tye (✉)
Department of Molecular Biology and Genetics, College of Agriculture and Life Sciences, Cornell University, Ithaca, NY, USA

Division of Life Science, Hong Kong University of Science and Technology, Hong Kong, China
e-mail: biktye@ust.hk

H. Masai, M. Foiani (eds.), *DNA Replication*, Advances in Experimental Medicine and Biology 1042, https://doi.org/10.1007/978-981-10-6955-0_9

9.1 Introduction

Of the three macromolecule-synthesizing machines that synthesize proteins, mRNAs and DNA, respectively, the crystal structures of the ribosome (Ramakrishnan 2010; Steitz 2010; Yonath 2010) and RNA polymerase (Kornberg 2007) have been determined at atomic resolution, and Nobel prizes were even awarded for these achievements. However, the replisome and many of its integral components have been recalcitrant to crystallization, and structural determination of the replisome has lagged behind. The replisome is a complex machine with multiple engines including a DNA-unwinding helicase at the front end and one leading-strand and two lagging-strand DNA polymerases chugging along at the back end. The size, asymmetry, flexibility, and multipartite nature of the replisome have posed difficult challenges for structural biologists on the mission to unravel its anatomical secrets. However, the prospects for unraveling the atomic structure of the replisome soon will change because of the advent of the cryo-EM revolution that took place in 2013 (Fernandez-Leiro and Scheres 2016). To date, two major structures that are critical for unraveling the anatomy of the helicase component of the replisome have been determined at near-atomic resolution. The first is the inactive MCM double hexamer determined at an overall resolution of 3.8 Å (Li et al. 2015). The unprecedented resolution achieved in this study lays a strong foundation for structural work on the helicase component of the replisome and will serve as a template for subsequent atomic modeling of all MCM-associated DNA replication complexes. The second is the CMG helicase resolved at a slightly lower resolution by two groups (Abid Ali et al. 2016; Yuan et al. 2016). In this chapter, we will focus on the structure and structure-informed functions of the MCM double hexamer. In the following chapter, the structure of the CMG helicase and the architecture of the replisome will be reviewed.

The Mcm2-7 hexameric complex is the core of the inactive MCM replication licensing complex (Tye 1999a; Donovan et al. 1997; Chong et al. 1995; Thommes et al. 1997) and the catalytic core of the Cdc45-MCM-GINS replicative helicase (Labib et al. 2000; Moyer et al. 2006; Gambus et al. 2006; Ilves et al. 2010). Three of the MCM subunits (Mcm2, Mcm3, and Mcm5) were initially identified in a yeast mutant hunt for proteins that regulate the initiation step of DNA replication (Tye 1999a). This screen utilized the maintenance of minichromosomes as an assay and hence the name (Maine et al. 1984; Tye 1999b). Paralogs of these Mcm proteins were subsequently identified in the yeasts and other eukaryotes from screens not necessarily related to DNA replication functions (Moir et al. 1982; Johnston and Thomas 1982; Bae et al. 2009). There is a total of eight Mcm paralogs. Mcm8 and Mcm9 are only found in metazoans, and their functions are less well known (Maiorano et al. 2005; Gambus and Blow 2013; Lutzmann et al. 2005; Nishimura et al. 2012; Traver et al. 2015). Mcm2, Mcm3, Mcm4, Mcm5, Mcm6, and Mcm7 form a hexameric complex that is involved in replication initiation and elongation in all eukaryotes (Bochman and Schwacha 2009). However, purified Mcm2-7 complexes show little or no helicase activity unless provided with the accessory factors, the tetrameric GINS and Cdc45 (Bochman and Schwacha 2008; Ilves et al. 2010).

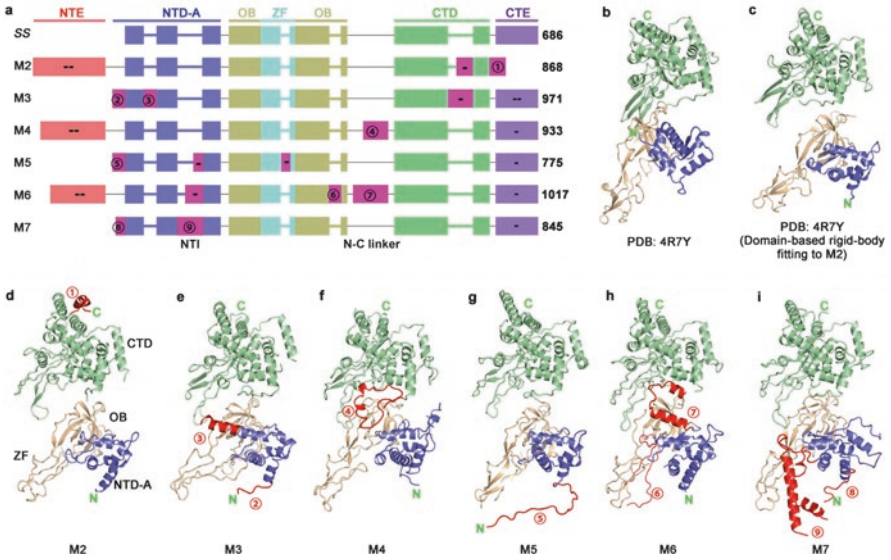

Fig. 9.1 Structural organization of the MCM2-7 subunits. **a** Schematic illustration of domain organization and subunit-specific features of MCM2-7 subunits, with comparison to the archaeal MCM (SS, *Sulfolobus solfataricus*). Numbered regions correspond to numbered extensions and insertions highlighted in (**d–i**). "-" symbols denote corresponding regions with reliable densities to trace the main-chain direction, but not sufficient for atomic modeling. "--" symbols denote sequences with highly disordered densities. (**b, c**) A protomer of the crystal structure of a chimeric archaeal MCM hexamer structure (PDB code 4R7Y) was used as the template for modeling with its subdomains divided and colored. The archaeal MCM was aligned globally (**b**) or domain-based flexibly fitted (**c**) to the atomic model of Mcm2. (**d–i**) Side-by-side structural comparison of MCM2-7 proteins, with Mcm3-7 globally aligned to the atomic model of Mcm2. The well-resolved insertions and extensions of each MCM subunit (**d–i**) are numbered and colored in *red* (Reproduced from Li et al. 2015)

In contrast, in archaebacteria, a single Mcm protein forms a homohexameric ring that displays robust helicase activity (Kelman et al. 1999; Chong et al. 2000). An alignment of the Mcm2, 3, 4, 5, 6, 7 amino acid sequence with their archaeal homologue shows that the CTD catalytic core and NTD core are highly conserved (Fig. 9.1a). Each of the Mcm2-7 subunit has its own characteristic CTE, NTI, and NTE that suggest subunit-specific functions.

The assembly and activation of Mcm2-7 helicases at replication origins are strictly regulated during each cell division cycle, ensuring replication initiation to occur at each origin no more than once (Diffley et al. 1994; Siddiqui et al. 2013). Several laboratories have been able to reconstitute the DNA replication system using purified yeast proteins (Georgescu et al. 2015; Yeeles et al. 2015). These laboratories have taken the approach to look at in vitro assembled replication complexes by negative staining EM and cryo-EM (Remus et al. 2009; Costa et al. 2011, 2014; Sun et al. 2013, 2014, 2015; Yuan et al. 2016; Abid Ali et al. 2016). An alternative approach is

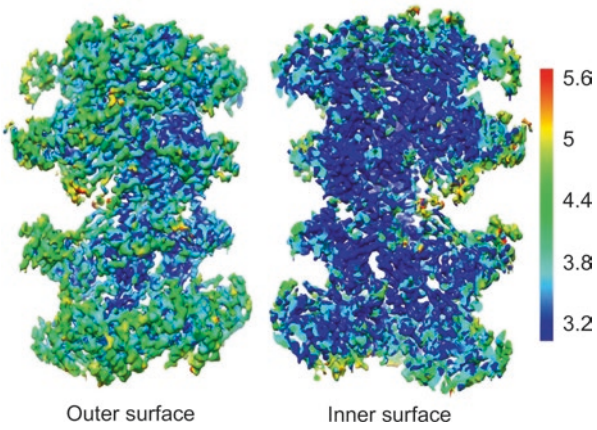

Fig. 9.2 The density map of the MCM2-7 double hexamer (sharpened) is shown in two views for the outer and inner surfaces. The map is color-coded to indicate the range of the local resolution

to purify endogenously assembled DNA replication complexes that may have a better chance of preserving fidelity but may compromise on the yield of such preparations.

In yeast, the soluble form of the Mcm2-7 complex is a single hexamer, and the chromatin-bound form of the complex is a double hexamer. Tye and collaborators purified the soluble single hexamer (SH) from an overexpression strain and the double hexamer (DH) from native chromatin and examined their structures by cryo-EM (Li et al. 2015). After much effort, they were unable to get a respectable 3-D structure of the SH because of its flexibility and instability. In contrast, the double hexamer was clearly much more stable. After only two sessions of data collection, a refined 3-D structure of the DH was obtained with a resolution of about 4.4 Å for the more flexible exterior and a better than 3.2 Å for the interior core (Fig. 9.2). The high quality of this EM density map allowed the assignment of each of the MCM subunits unambiguously without the help of conventional tagging strategy (Figs. 9.1d–i and 9.3c–e). The crystal structure of the conserved core region of the chimera of *Sulfolobus solfataricus* NTD and *Pyrococcus furiosus* CTD (Fig. 9.1b) (Miller et al. 2014) was used for the atomic modeling. Rigid body domains of the chimera were divided into four segments (NTD-A, OB-fold, ZF, and CTD) and fitted onto the electron density map with manual adjustments according to predicted secondary structures (Fig. 9.1b–i). For regions without a known template, the model relied on predicted secondary structure and tracing of the main chain based solely on densities. As a result, an atomic model of the DH for ~80% of its sequence, including most of the subunit-specific extensions and insertions, was built.

9.2 Asymmetry of the Double Hexamer

The double hexamer is a rigid, head-to-head double ring structure that is slightly tilted, twisted, and offset with respect to each other, similar to that described previously for in vitro purified DH (Sun et al. 2014). The relative positions of the subunits

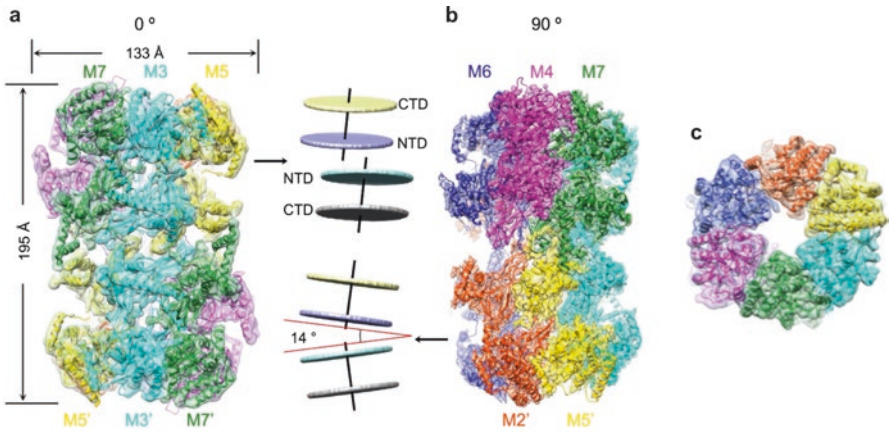

Fig. 9.3 Overall structure of the MCM2-7 double hexamer. (**a–c**) Side (**a, b**) and *top* (**c**) views of the cryo-EM map of the MCM2-7 DH purified from native chromatin (Reproduced from Li et al. 2015). The map is superimposed with the atomic model. Unsharpened map (**a**) is displayed from the twofold axis, and sharpened map (**b**) is displayed with indicated rotations relative to **a** along the cylinder axis. The tilted and twisted arrangements of the two single hexamers are illustrated in the side panels of (**a**, **b**)

were also in the precise predicted order determined by low-resolution cryo-EM except that the assignment of the CTD relative to the NTD was different. In the atomic model, the CTD is almost vertically aligned with respect to the NTD (Fig. 9.3) rather than the sharp anticlockwise displacement in the earlier model. The top view from the CTD shows a compact closed ring with an open channel wide enough for dsDNA to pass through without the obstructions of the CTE reported in Sun et al. (2014). These observed differences could result from in vitro versus in vivo assembly.

The tilted arrangement of the two SHs forms a 14° wedge in between (Fig. 9.3). The Mcm2/Mcm6/Mcm4 subunits from both SHs are all positioned at the thick edge. Although the very long NTEs from Mcm2, Mcm4, and Mcm6 (Fig. 9.1a) appear too disordered to produce observable electron density, their bulkiness is believed to be the cause of the tilted conformation of the DH. The localization of these three subunits at the thick edge of the DH wedged site allows an increased opening between the two hexamers and thus a solvent exposure of their NTEs. Notably, they are side by side on one SH and head-to-head on the DH (Fig. 9.3), and hence, a large surface area on top of six NTEs from two hexamers virtually forms a docking platform for regulatory kinases such as DDK during helicase activation. Consistent with this notion, the NTEs of Mcm2 (Lei et al. 1997), Mcm4, and Mcm6 (Sheu and Stillman 2006; Randell et al. 2010) are known substrates of DDK, and the DH, but not the SH, is the preferred substrate for DDK (Sun et al. 2014). In vitro assembly assays indicate that phosphorylated DH supports initial recruitment of Sld3 and Cdc45 (Deegan et al. 2016), followed by GINS and further phosphorylation by CDK, to form a functional CMG helicase for DNA unwinding (Yeeles et al. 2015; Heller et al. 2011). Low-resolution EM studies showed that DDK phosphorylation neither triggers the

uncoupling of the DH nor causes conformational change in its overall structure (On et al. 2014; Sun et al. 2014). However, subtle alterations in DH structure induced by DDK may be critical for the transformation of the inactive DH into the active CMG helicases via Mcm2/Mcm5 gate opening and/or DH uncoupling. High-resolution structure determination of the phosphorylated DH using advanced cryo-EM analysis may provide insight into this intricate pivotal mechanism.

9.3 Tight Junction at the NTDs

Archaeal homohexameric MCM complex can form DH in solution directly through head-to-head interactions between zinc finger motifs from opposite hexamers (Chong et al. 2000; Brewster et al. 2008). In contrast, the eukaryotic heterohexameric Mcm2-7 can only be assembled into a dimer of hexamers on duplex origin DNA (Remus et al. 2009; Evrin et al. 2009). Furthermore, this assembly process is tightly controlled in a stepwise manner. The Mcm2-7 hexamer is recruited to the ORC-Cdc6-binding site during the G1 phase one at a time (Ticau et al. 2015; Sun et al. 2014). Once assembled, the Mcm2-7 hexamers form a topologically stable, inactive head-to-head double hexamer that encircles duplex origin DNA (Remus et al. 2009). The assembly of the double hexamer is an energy-consuming process requiring the hydrolysis of ATP by both ORC-Cdc6 and Mcm2-7 during the loading of the first and the second hexamer (Coster et al. 2014; Kang et al. 2014). Similar to archaeal DH formation, interactions among ZF motifs from Mcm2-7 subunits contribute to the stabilization of DH. However, unlike the simple head-on interactions between ZFs from two archaeal SHs, the inter-ZF interactions of eukaryotic Mcm2-7 appear to be more versatile, forming additional interactions with NTEs and β turns of the opposing hexamer in some cases (Fig. 9.4). This elaborate intertwining and extensions of NTEs into the opposite hexamers suggest that formation of the head-to-head tight junction is an ATP-consuming process that requires partial unfolding of the NTDs before forming the rigid interlocked structure.

Due to the tilted and twisted arrangement of the two SHs, the orientations of ZFs are completely different at two sides of the wedged interface of the DH: vertical at the thick Mcm2/Mcm6/Mcm4 side and horizontal at the thin Mcm5/3/7 side. This unique arrangement ensures intimate contacts among ZFs. In addition, according to the buried surface calculated at the hexamer interface, NTDs, NTEs, and NTIs from Mcm5/3/7 play significant roles in contributing to a stable DH (Fig. 9.4), which is even greater than ZF interactions. The involvement of NTEs of Mcm2/Mcm6/Mcm4 in stabilizing DH remains unknown because of their highly disordered feature in the structure. More importantly, although N-terminal sequences of each MCM subunits are less conserved in higher eukaryotes, most of the NTDs, NTEs, and NTIs (mainly NTI of M7, NTE of M5, β-turn of M6) involved in inter-hexamer interactions are conserved, suggesting the inter-subunit interactions are most likely maintained in metazoans as well.

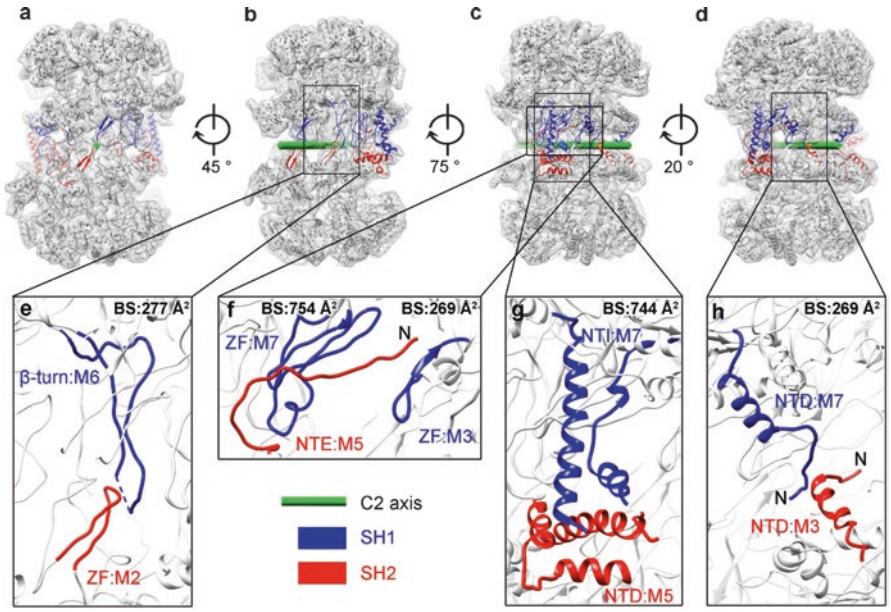

Fig. 9.4 Stabilization of MCM2-7 double hexamer contributed by NTEs and NTIs. (**a–d**) Side views of the MCM2-7 DH, with indicated rotations around the cylinder axis. Atomic structure is superimposed with the unsharpened map. The sequence elements involved in inter-hexamer interactions are highlighted. (**e–h**) Zoomed-in views of the boxed regions from (**b–d**). Buried areas (Å^2) of these interfaces in (**e–h**) are labeled. BS, buried surface (Reproduced from Li et al. 2015)

The tight coupling of the double hexamer at the NTD raises the question of how the two hexamers uncouple upon helicase activation. In vitro reconstitution and genetic analysis show that separation of MCM DH in S phase involves the engagement of other initiation factors such as Cdc45, GINS, and Mcm10 to unravel the entanglement between the NTDs and NTIs of M5, M3, and M7. Consistent with this idea, recent CMG structure showed that two α-helices of Psf2 interact with NTD of Mcm5 (Abid Ali et al. 2016; Yuan et al. 2016) which is contacted by the NTE of the opposite Mcm7 in the DH. Previous study also showed that Cdc45 can interact with Mcm5-N (N-terminus) and Mcm2-N and Psf2 with Mcm5-N and Psf3 with Mcm3-N(Costa et al. 2011; Yuan et al. 2016; Abid Ali et al. 2016); in addition, Mcm10 has been shown to interact physically with MCM6 (van Deursen et al. 2012) and MCM7 (Homesley et al. 2000). Presumably these factors work cooperatively to uncouple the MCM DH. The recruitment of all these factors requires the action of DDK and CDKs during S phase to ensure the sequential coupling and uncoupling of the MCM hexamers at separate stages of each cell division cycle (Heller et al. 2011; Yeeles et al. 2015). Again, the role of DDK phosphorylation in triggering the DH uncoupling is still unclear. A better understanding of this process will rely on the determination of the atomic structures of the intermediate replication complexes during helicase activation and the delineation of conformational changes induced by the uncoupling factors.

9.4 A Unique Side Channel at the Mcm2-Mcm6 Interface

The archaeal MCM helicase is made up of six identical subunits, which form a ring with six identical interfaces (Bochman and Schwacha 2009). The atomic model of the archaeal MCM helicase built from the crystal structure of the near-full-length protomer of the ssoMCM by applying a sixfold symmetry showed six side channels at the neck region of the ring (Brewster et al. 2008). The size of the side channels large enough for ssDNA to pass through raised speculations that dsDNA may pass through the central channel at the CTD and unwound by extrusion of one strand laterally at the side channel. This configuration would favor the strand extrusion model for DNA unwinding. Throughout the years, this model has been disfavored based on in vitro biochemical studies using bulky chemical crosslinks on the leading and lagging strands (Fu et al. 2011). The CMG helicase efficiently bypasses a roadblock embedded on the lagging strand more efficiently than that embedded on the leading strand, arguing against the translocation of CMG helicase on dsDNA. Most recently, the structure of the apo CMG helicase has been determined by cryo-EM (Yuan et al. 2016). The WH domain of Mcm5 restricts the main channel of the CMG helicase to the extent that only ssDNA can be accommodated. The positions of the ssDNA associated with the CMG are consistent with the steric exclusion model in which duplex DNA is unwound by the translocation of the CMG on ssDNA.

The observation that the yeast MCM double hexamer contains a central channel that can accommodate dsDNA and a side channel between Mcm2 and Mcm6 wide enough to accommodate ssDNA (Fig. 9.5a) encourages a revisit of the strand extrusion model. Despite all the evidence against this model, it is worthwhile to reevaluate the evidence. First, the in vitro roadblock bypass experiment showed only a bias in the efficiency of bypass rather than a clear-cut bypass on the lagging strand but not the leading strand. Also, the latching of the Mcm2-Mcm5 gate by GINS and Cdc45 in the CMG helicase structure suggests that the gate is only loosely fastened and may not be closed shut or irreversibly latched on during translocation (Costa et al. 2011, 2014). As for the threading of the artificial Y-shaped DNA substrate through the in vitro assembled CMG helicase, it may not correctly represent how DNA is threaded in a CMG helicase assembled de novo at replication origins. Most interestingly, a recent model for the architecture of the in vitro assembled core replisome suggests that DNA polymerase epsilon is placed ahead of the helicase on the leading strand (Sun et al. 2015). Although the path of the DNA could not be traced, the position of Polε would require a sharp U-turn in the threading of the leading strand from the NTD of the CMG helicase to the DNA polymerase if the steric exclusion model is correct (Fig. 9.5b). Indeed, without the evidence of an atomic structure of an endogenous replisome, one can easily come up with radical models that are more compatible with the positioning of Polε by using the unique side channel (Fig. 9.5c). In this model, the side channel would act like a plowshare to force apart the two strands as the helicase plows ahead. Whether the CMG helicase unwinds DNA by strand extrusion, steric exclusion or some other mechanisms remains to be verified by cryo-EM structures of CMG helicase assembled from replication origins.

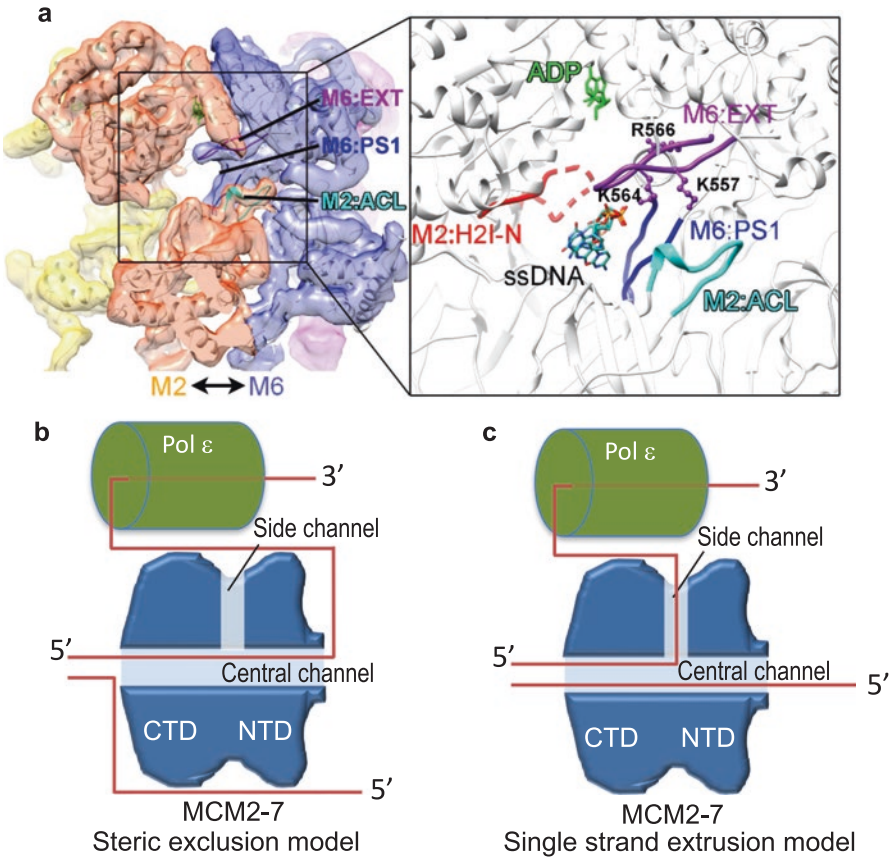

Fig. 9.5 A unique side channel between Mcm2 and Mcm6. **a** Outer surface representation of the Mcm2/Mcm6 interface. The boxed region is shown in a zoomed-in view (*right*) with individual components (H2I-N, EXT, PS1, and ACL) colored individually. A short piece of ssDNA is modeled in the structure to indicate the size of this side channel large enough to act as a pore for strand extrusion from the central channel during DNA unwinding along with basic residues (Arg566, Lys557, and Lys564) of the EXT hairpin from MCM6. The H2I-N is partially disordered. (**b, c**) Threading paths proposed for leading- and lagging-strand DNA based on the architecture of the replisome (Sun et al. 2015) in the steric exclusion model (**b**) versus the strand extrusion model where the 3′-5′ strand extrudes through Mcm2/Mcm6 side channel (**c**)

9.5 ATPase Pockets in the Double Hexamer

Mcm2-7 forms the core of the replication-licensing complex that assembles the replication initiation complex at replication origins and the core of the replicative helicase that unwinds dsDNA at replication forks (Bochman and Schwacha 2009). In both capacities, ATP hydrolysis by the Mcm2-7 catalytic core is required to fuel the energy-consuming functions that it performs.

Heterohexameric Mcm2-7 belongs to the AAA+ family of ATPases, whose ATPase active sites are formed at inter-subunit interfaces. One subunit contributes the Walker A and B motifs, while the other contributes the arginine finger. Thus, each Mcm subunit participates in two ATPase active sites, resulting in six distinct ATPase pockets. At each step of the assembly, starting from the single hexamers to the pre-RC and then from the pre-RC to the pre-IC, a different set of ATPases is called into action. Exhaustive mutant and biochemical analysis combined with in vitro reconstitution studies was able to identify which ATPase pocket is required for activity at each assembly step (Bochman and Schwacha 2008; Coster et al. 2014; Kang et al. 2014). Figure 9.6g (modified from Kang et al. 2014) summarizes the results of these elegant and intricate studies that show which ATPase pocket(s) is required at each stage. During this process, the 2:6 ATPase appears to play a role in the loading of the first SH. The 4:7, 6:4, 5:2, and 3:5 ATPases are required for the loading and head-to-head fusion of the second SH to form the DH. Up to this point, the only ATPase pocket that is not required for activity is the 7:3 pocket as if all of the energy consumed up to this point is to assemble this high-energy structure that is stable throughout G1 phase. Interestingly, in the high-resolution structure of the inactive DH, only the 7:3 ATPase pocket shows extra density indicating the possibility of ATP bound (Fig. 9.6a–f) (Li et al. 2015). It would be interesting to find out what exactly happens in the steps that follow. For example, is ATP hydrolysis by the 7:3 pocket the first responder of DDK or CDK phosphorylation to initiate DNA melting at the G1-S phase transition, which in turn recruits Sld3 and Cdc45? According to the in vitro reconstitution study, all of the ATPases except 6:4 act immediately after the CDK action to recruit GINS and RPA (Kang et al. 2014). What seems remarkable is how the asymmetry of the MCM ATPase pockets directs the sequential assembly of the replication initiation complex to form the helicase engine of the replisome. However, to unravel which ATPase is called into action at which specific step would require the high-resolution structure of each staged assembly that shows the nucleotide-binding state of each ATPase pocket as achieved for the double hexamer (Li et al. 2015). The double hexamer is an unusually stable structure that can withstand washing by 0.5 M salt (Bowers et al. 2004; Remus et al. 2009; Evrin et al. 2009) and therefore more amenable to structural analysis. It may be difficult to find stable conditions for each of the intermediate assembly structures for high-resolution structural analysis.

As a footnote to the importance of high-resolution structures, a previous study using negative staining EM suggested that the inactivation of the ATPase pocket in the DH is due to the uncoupling of the ATP hydrolysis motifs by the staggering of the CTD and NTD of each subunit (Sun et al. 2014). It should be pointed out that the model presented was based on the misassignment of the CTDs of the subunits that led the authors to these conclusions.

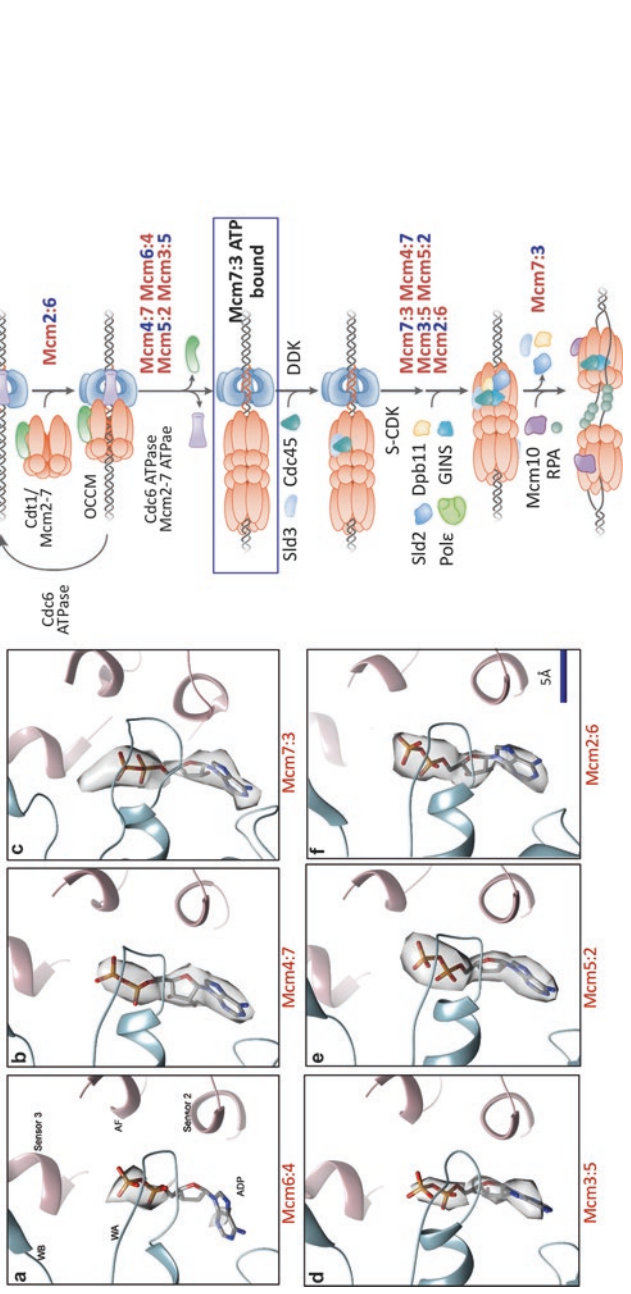

Fig. 9.6 MCM2-7 ATPase pockets involved in different stages of helicase loading and activation. (**a**–**f**) Zoomed-in views of nucleotide occupancy at the six ATPase centers of MCM2-7 double hexamer. The conserved ATPase elements of the active centers are labeled as in (**a**). Segmented nucleotide densities at a contour level of 5.5σ were superimposed (transparent gray). Nucleotides were modeled using ADP (Reproduced from Li et al. 2015). (**g**) Kang et al. (2014) purified a series of Cdt1-MCM2-7 heptamers to examine the role of each MCM2-7 ATPase active site during DNA replication initiation. Each complex contains a single mutation in either Walker A (K to A) or arginine finger (R to A) motif of a particular Mcm subunit. The identified ATPase active sites are summarized in this cartoon. McmX:X in which number highlighted in blue represents the subunit location of that single mutation: left, Walker A motif, and right, arginine finger motif (Adapted from Kang et al. (2014) Fig. 7 by permission from Elsevier publisher Inc. copyright 2014). The unique ATP-bound state of the 7:3 ATPase in the DH atomic model is highlighted by a *boxed* frame

9.6 Central Channel and Model of Initial Origin Melting

Like many hexameric AAA+ machineries (Brewster et al. 2010; Enemark and Joshua-Tor 2006), Mcm2-7 complex also has a central-pored chamber decorated by multiple layers of hairpin loops formed by the H2Is and β-turn motifs from the OB domains. These motifs are placed in axially staggered positions, resembling archaeal MCM structures in contacting with ssDNA and dsDNA (Miller et al. 2014). The atomic model for the DH suggests that MCM2-7 helicase employs a similar mechanism in controlling the axial displacement of these loops to facilitate DNA translocation and unwinding (Fig. 9.7a, b).

The most striking feature of the MCM2-7 DH structure is that the central channel, formed by these two staggered MCM rings, has four constriction points in the channel and a kink at the interface of the two rings (Fig. 9.7a, b). Modeling with dsDNA shows that these constriction points interact with the major and minor grooves of dsDNA consistent with observations that the DH complexes stably associate with linear dsDNA under physiological condition and only becomes mobile on dsDNA in high-salt buffer (Remus et al. 2009; Kumar and Remus 2016). These fine structures of the MCM2-7 DH provide insight into its function in DNA melting (Fig. 9.8). First, the kinked interface of the two rings would deform dsDNA (Fig. 9.7e), which could serve as a nucleation center for DNA destabilization. It has been shown that DNA bending that distorts hydrogen bonds between base pairs causes local DNA melting and facilitates DNA unwinding during transcription (Tang and Patel 2006). Second, the tight grip of duplex DNA by the two restriction points in the two SH chambers would further deform DNA at the nucleation point if rotated against each other. Third, possible rotations between ring structures formed by subdomains of each hexamer would lower the activation energy for DNA destabilization even fur-

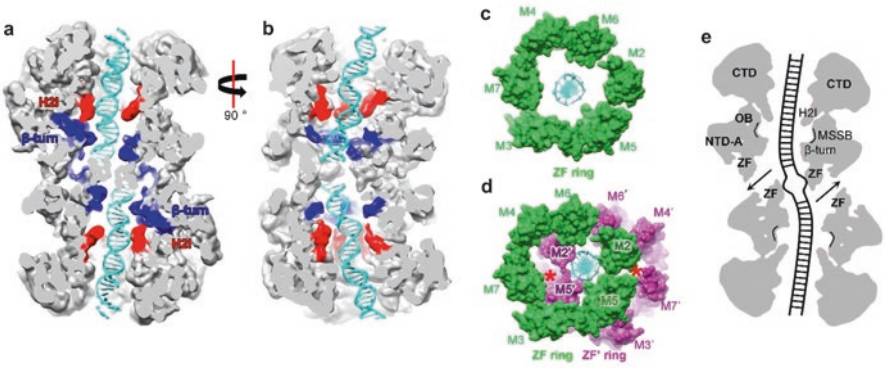

Fig. 9.7 Central channel and its implication in origin melting. (**a, b**) Cutaway views of the density map (unsharpened) with two dsDNA fragments fitted in the central channel. Surface representation of the atomic models of ZFs from one single hexamer (**c**) and ZFs from both single hexamers (**d**). (**e**) A simplified diagram of the cryo-EM map of the MCM2-7 DH. The structural features that may involve in the initial melting step are labeled as indicated (Reproduced from Li et al. 2015)

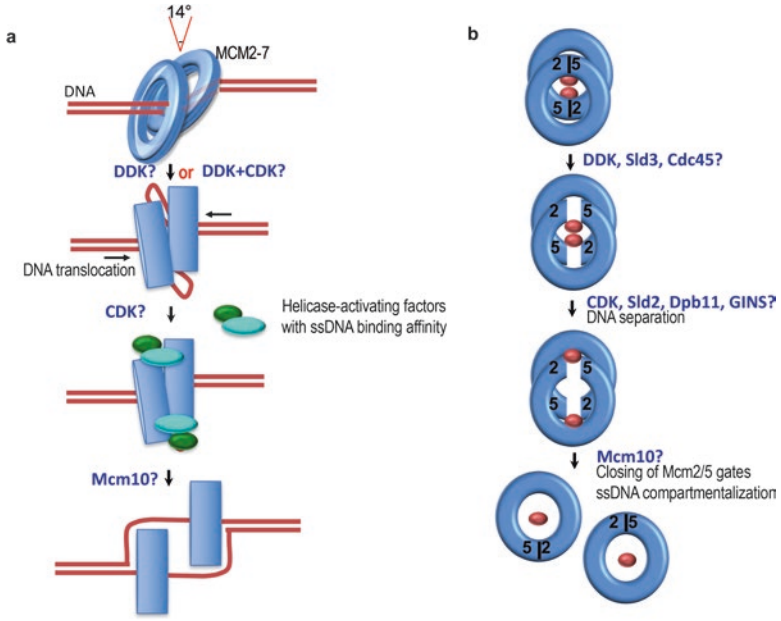

Fig. 9.8 A model for gate opening and initial DNA melting during helicase activation. Although many factors have been shown to be required for this process, it is unclear when and how they are involved in the actual gate opening and DNA melting events. See text for details

ther. Recent single-molecule analysis of *Dm*CMG helicase showed that the CTD and NTD of the DmCMG helicase could rotate in opposite directions, clockwise and anticlockwise, during its engagement with DNA (Abid Ali et al. 2016). These special features of the atomic model of the DH suggest that allosteric conformational changes following the activation of the MCM2-7 complex by cell cycle-regulated kinases might bring about DNA destabilization for initial DNA melting.

Another notable feature about the DH structure is that the overlapping of two central channels at the interface forms a narrowed main channel and two minor or exit channels. Interestingly, the main channel is formed mostly by two ZF pairs from the gate-forming subunits Mcm2 and Mcm5 (Fig. 9.7c, d). The size of the main channel is just wide enough to fit dsDNA. However, once the Mcm2/Mcm5 gates are opened at the interface region, the three channels would join together to form a space large enough for strand separation (Fig. 9.8b). Strand separation is likely assisted by the MSSB motifs conveniently located on opposite sides of the enlarged chamber (Fig. 9.7e) (Miller et al. 2014). During this DNA melting step, if the two MCM hexamers fused at the NTDs translocate along dsDNA in opposite directions, they will effectively pump in dsDNA from both ends. The already deformed DNA at the kink region would be subsequently separated (Fig. 9.8b). The melted single-DNA strands that become accessible to the outside by looping out from the exit channels could be captured by helicase-activating factors to secure their separation (Fig. 9.8a). Several of the helicase-activating factors, such as Sld2,

Sld3, Cdc45, and Mcm10, have been shown to have ssDNA-binding property (Bruck and Kaplan 2011, 2013; Costa et al. 2014; Homesley et al. 2000; Eisenberg et al. 2009). At the final step, which is yet to be understood, the DH is uncoupled, and the lagging-strand DNA is excluded from each of the MCM hexameric ring (Yardimci et al. 2010; Fu et al. 2011).

9.7 Looking Ahead

Despite the many hurdles that have held back fine-detailed structural studies of the DNA replication machinery, there is reason for optimism for unraveling this last macromolecule-synthesizing machine in the near future. Determining the near-atomic resolution structure of the inactive MCM double hexamer is a crucial start of this endeavor. The Mcm2-7 complex is a major player throughout the entire process of DNA replication, from replication licensing to initial melting of origin DNA, progression of bidirectional forks, and finally replication termination (Bell and Labib 2016). In each step, the MCM complex appears to play a somewhat different role first as an inert assembly platform, and then a duplex DNA pump, a translocator on ssDNA, and finally, a disbander of the replisome. The recent advances in cryo-EM promise that the determination of many of these MCM-associated structures is at hand. Combined with single-molecule studies and the in vitro reconstitution of the stepwise-assembled intermediates of the replisome, the next decade will witness the visualization of the workings of the replisome that is so vividly portrayed in textbooks from elegant biochemical and genetic studies of decades before.

References

Abid Ali F, Renault L, Gannon J, Gahlon HL, Kotecha A, Zhou JC, Rueda D, Costa A (2016) Cryo-EM structures of the eukaryotic replicative helicase bound to a translocation substrate. Nat Commun 7:10708. https://doi.org/10.1038/ncomms10708

Bae B, Chen YH, Costa A, Onesti S, Brunzelle JS, Lin Y, Cann IK, Nair SK (2009) Insights into the architecture of the replicative helicase from the structure of an archaeal MCM homolog. Structure 17(2):211–222. https://doi.org/10.1016/j.str.2008.11.010

Bell SP, Labib K (2016) Chromosome duplication in Saccharomyces cerevisiae. Genetics 203(3):1027–1067. https://doi.org/10.1534/genetics.115.186452

Bochman ML, Schwacha A (2008) The Mcm2-7 complex has in vitro helicase activity. Mol Cell 31(2):287–293. https://doi.org/10.1016/j.molcel.2008.05.020

Bochman ML, Schwacha A (2009) The Mcm complex: unwinding the mechanism of a replicative helicase. Microbiol Mol Biol Rev: MMBR 73(4):652–683. https://doi.org/10.1128/MMBR.00019-09

Bowers JL, Randell JC, Chen S, Bell SP (2004) ATP hydrolysis by ORC catalyzes reiterative Mcm2-7 assembly at a defined origin of replication. Mol Cell 16(6):967–978. https://doi.org/10.1016/j.molcel.2004.11.038

Brewster AS, Wang G, Yu X, Greenleaf WB, Carazo JM, Tjajadi M, Klein MG, Chen XS (2008) Crystal structure of a near-full-length archaeal MCM: functional insights for an AAA+ hexa-

meric helicase. Proc Natl Acad Sci U S A 105(51):20191–20196. https://doi.org/10.1073/pnas.0808037105

Brewster AS, Slaymaker IM, Afif SA, Chen XS (2010) Mutational analysis of an archaeal mini-chromosome maintenance protein exterior hairpin reveals critical residues for helicase activity and DNA binding. BMC Mol Biol 11:62. https://doi.org/10.1186/1471-2199-11-62

Bruck I, Kaplan DL (2011) Origin single-stranded DNA releases Sld3 protein from the Mcm2-7 complex, allowing the GINS tetramer to bind the Mcm2-7 complex. J Biol Chem 286(21):18602–18613. https://doi.org/10.1074/jbc.M111.226332

Bruck I, Kaplan DL (2013) Cdc45 protein-single-stranded DNA interaction is important for stalling the helicase during replication stress. J Biol Chem 288(11):7550–7563. https://doi.org/10.1074/jbc.M112.440941

Chong JP, Mahbubani HM, Khoo CY, Blow JJ (1995) Purification of an MCM-containing complex as a component of the DNA replication licensing system. Nature 375(6530):418–421. https://doi.org/10.1038/375418a0

Chong JP, Hayashi MK, Simon MN, Xu RM, Stillman B (2000) A double-hexamer archaeal minichromosome maintenance protein is an ATP-dependent DNA helicase. Proc Natl Acad Sci U S A 97(4):1530–1535. https://doi.org/10.1073/pnas.030539597

Costa A, Ilves I, Tamberg N, Petojevic T, Nogales E, Botchan MR, Berger JM (2011) The structural basis for MCM2-7 helicase activation by GINS and Cdc45. Nat Struct Mol Biol 18(4):471–477. https://doi.org/10.1038/nsmb.2004

Costa A, Renault L, Swuec P, Petojevic T, Pesavento JJ, Ilves I, MacLellan-Gibson K, Fleck RA, Botchan MR, Berger JM (2014) DNA binding polarity, dimerization, and ATPase ring remodeling in the CMG helicase of the eukaryotic replisome. elife 3:e03273. https://doi.org/10.7554/eLife.03273

Coster G, Frigola J, Beuron F, Morris EP, Diffley JF (2014) Origin licensing requires ATP binding and hydrolysis by the MCM replicative helicase. Mol Cell 55(5):666–677. https://doi.org/10.1016/j.molcel.2014.06.034

Deegan TD, Yeeles JT, Diffley JF (2016) Phosphopeptide binding by Sld3 links Dbf4-dependent kinase to MCM replicative helicase activation. EMBO J 35(9):961–973. 10.15252/embj.201593552

van Deursen F, Sengupta S, De Piccoli G, Sanchez-Diaz A, Labib K (2012) Mcm10 associates with the loaded DNA helicase at replication origins and defines a novel step in its activation. EMBO J 31(9):2195–2206. https://doi.org/10.1038/emboj.2012.69

Diffley JF, Cocker JH, Dowell SJ, Rowley A (1994) Two steps in the assembly of complexes at yeast replication origins in vivo. Cell 78(2):303–316

Donovan S, Harwood J, Drury LS, Diffley JF (1997) Cdc6p-dependent loading of Mcm proteins onto pre-replicative chromatin in budding yeast. Proc Natl Acad Sci U S A 94(11):5611–5616

Eisenberg S, Korza G, Carson J, Liachko I, Tye BK (2009) Novel DNA binding properties of the Mcm10 protein from Saccharomyces cerevisiae. J Biol Chem 284(37):25412–25420. https://doi.org/10.1074/jbc.M109.033175

Enemark EJ, Joshua-Tor L (2006) Mechanism of DNA translocation in a replicative hexameric helicase. Nature 442(7100):270–275. https://doi.org/10.1038/nature04943

Evrin C, Clarke P, Zech J, Lurz R, Sun J, Uhle S, Li H, Stillman B, Speck C (2009) A double-hexameric MCM2-7 complex is loaded onto origin DNA during licensing of eukaryotic DNA replication. Proc Natl Acad Sci U S A 106(48):20240–20245. https://doi.org/10.1073/pnas.0911500106

Fernandez-Leiro R, Scheres SHW (2016) Unravelling biological macromolecules with cryo-electron microscopy. Nature 537(7620):339–346. https://doi.org/10.1038/nature19948

Fu YV, Yardimci H, Long DT, Ho TV, Guainazzi A, Bermudez VP, Hurwitz J, van Oijen A, Scharer OD, Walter JC (2011) Selective bypass of a lagging strand roadblock by the eukaryotic replicative DNA helicase. Cell 146(6):931–941. https://doi.org/10.1016/j.cell.2011.07.045

Gambus A, Blow JJ (2013) Mcm8 and Mcm9 form a dimeric complex in Xenopus laevis egg extract that is not essential for DNA replication initiation. Cell Cycle 12(8):1225–1232. https://doi.org/10.4161/cc.24310

Gambus A, Jones RC, Sanchez-Diaz A, Kanemaki M, van Deursen F, Edmondson RD, Labib K (2006) GINS maintains association of Cdc45 with MCM in replisome progression complexes at eukaryotic DNA replication forks. Nat Cell Biol 8(4):358–366. https://doi.org/10.1038/ncb1382

Georgescu RE, Schauer GD, Yao NY, Langston LD, Yurieva O, Zhang D, Finkelstein J, O'Donnell ME (2015) Reconstitution of a eukaryotic replisome reveals suppression mechanisms that define leading/lagging strand operation. elife 4:e04988. https://doi.org/10.7554/eLife.04988

Heller RC, Kang S, Lam WM, Chen S, Chan CS, Bell SP (2011) Eukaryotic origin-dependent DNA replication in vitro reveals sequential action of DDK and S-CDK kinases. Cell 146(1):80–91. https://doi.org/10.1016/j.cell.2011.06.012

Homesley L, Lei M, Kawasaki Y, Sawyer S, Christensen T, Tye BK (2000) Mcm10 and the MCM2-7 complex interact to initiate DNA synthesis and to release replication factors from origins. Genes Dev 14(8):913–926

Ilves I, Petojevic T, Pesavento JJ, Botchan MR (2010) Activation of the MCM2-7 helicase by association with Cdc45 and GINS proteins. Mol Cell 37(2):247–258. https://doi.org/10.1016/j.molcel.2009.12.030

Johnston LH, Thomas AP (1982) The isolation of new DNA synthesis mutants in the yeast Saccharomyces cerevisiae. Mol Gen Genet 186(3):439–444

Kang S, Warner MD, Bell SP (2014) Multiple functions for Mcm2-7 ATPase motifs during replication initiation. Mol Cell 55(5):655–665. https://doi.org/10.1016/j.molcel.2014.06.033

Kelman Z, Lee J-K, Hurwitz J (1999) The single minichromosome maintenance protein of Methanobacterium thermoautotrophicum ΔH contains DNA helicase activity. Proc Natl Acad Sci 96(26):14783–14788. https://doi.org/10.1073/pnas.96.26.14783

Kornberg R (2007) The molecular basis of eukaryotic transcription (Nobel lecture). Angew Chem 46(37):6956–6965. https://doi.org/10.1002/anie.200701832

Kumar C, Remus D (2016) Eukaryotic replication origins: strength in flexibility. Nucleus 7(3):292–300. https://doi.org/10.1080/19491034.2016.1187353

Labib K, Tercero JA, Diffley JF (2000) Uninterrupted MCM2-7 function required for DNA replication fork progression. Science 288(5471):1643–1647

Lei M, Kawasaki Y, Young MR, Kihara M, Sugino A, Tye BK (1997) Mcm2 is a target of regulation by Cdc7-Dbf4 during the initiation of DNA synthesis. Genes Dev 11(24):3365–3374

Li N, Zhai Y, Zhang Y, Li W, Yang M, Lei J, Tye BK, Gao N (2015) Structure of the eukaryotic MCM complex at 3.8 A. Nature 524(7564):186–191. https://doi.org/10.1038/nature14685

Lutzmann M, Maiorano D, Mechali M (2005) Identification of full genes and proteins of MCM9, a novel, vertebrate-specific member of the MCM2-8 protein family. Gene 362:51–56. https://doi.org/10.1016/j.gene.2005.07.031

Maine GT, Sinha P, Tye BK (1984) Mutants of S. cerevisiae defective in the maintenance of minichromosomes. Genetics 106(3):365–385

Maiorano D, Cuvier O, Danis E, Mechali M (2005) MCM8 is an MCM2-7-related protein that functions as a DNA helicase during replication elongation and not initiation. Cell 120(3):315–328. https://doi.org/10.1016/j.cell.2004.12.010

Miller JM, Arachea BT, Epling LB, Enemark EJ (2014) Analysis of the crystal structure of an active MCM hexamer. elife 3:e03433. https://doi.org/10.7554/eLife.03433

Moir D, Stewart SE, Osmond BC, Botstein D (1982) Cold-sensitive cell-division-cycle mutants of yeast: isolation, properties, and pseudoreversion studies. Genetics 100(4):547–563

Moyer SE, Lewis PW, Botchan MR (2006) Isolation of the Cdc45/Mcm2-7/GINS (CMG) complex, a candidate for the eukaryotic DNA replication fork helicase. Proc Natl Acad Sci U S A 103(27):10236–10241. https://doi.org/10.1073/pnas.0602400103

Nishimura K, Ishiai M, Horikawa K, Fukagawa T, Takata M, Takisawa H, Kanemaki MT (2012) Mcm8 and Mcm9 form a complex that functions in homologous recombination repair induced by DNA interstrand crosslinks. Mol Cell 47(4):511–522. https://doi.org/10.1016/j.molcel.2012.05.047

On KF, Beuron F, Frith D, Snijders AP, Morris EP, Diffley JF (2014) Prereplicative complexes assembled in vitro support origin-dependent and independent DNA replication. EMBO J 33(6):605–620. https://doi.org/10.1002/embj.201387369

Ramakrishnan V (2010) Unraveling the structure of the ribosome (Nobel lecture). Angew Chem 49(26):4355–4380. https://doi.org/10.1002/anie.201001436

Randell JC, Fan A, Chan C, Francis LI, Heller RC, Galani K, Bell SP (2010) Mec1 is one of multiple kinases that prime the Mcm2-7 helicase for phosphorylation by Cdc7. Mol Cell 40(3):353–363. https://doi.org/10.1016/j.molcel.2010.10.017

Remus D, Beuron F, Tolun G, Griffith JD, Morris EP, Diffley JF (2009) Concerted loading of Mcm2-7 double hexamers around DNA during DNA replication origin licensing. Cell 139(4):719–730. https://doi.org/10.1016/j.cell.2009.10.015

Sheu YJ, Stillman B (2006) Cdc7-Dbf4 phosphorylates MCM proteins via a docking site-mediated mechanism to promote S phase progression. Mol Cell 24(1):101–113. https://doi.org/10.1016/j.molcel.2006.07.033

Siddiqui K, On KF, Diffley JF (2013) Regulating DNA replication in eukarya. Cold Spring Harb Perspect Biol 5(9). https://doi.org/10.1101/cshperspect.a012930

Steitz TA (2010) From the structure and function of the ribosome to new antibiotics (Nobel lecture). Angew Chem 49(26):4381–4398. https://doi.org/10.1002/anie.201000708

Sun J, Evrin C, Samel SA, Fernandez-Cid A, Riera A, Kawakami H, Stillman B, Speck C, Li H (2013) Cryo-EM structure of a helicase loading intermediate containing ORC-Cdc6-Cdt1-MCM2-7 bound to DNA. Nat Struct Mol Biol 20(8):944–951. https://doi.org/10.1038/nsmb.2629

Sun J, Fernandez-Cid A, Riera A, Tognetti S, Yuan Z, Stillman B, Speck C, Li H (2014) Structural and mechanistic insights into Mcm2-7 double-hexamer assembly and function. Genes Dev 28(20):2291–2303. https://doi.org/10.1101/gad.242313.114

Sun J, Shi Y, Georgescu RE, Yuan Z, Chait BT, Li H, O'Donnell ME (2015) The architecture of a eukaryotic replisome. Nat Struct Mol Biol 22(12):976–982. https://doi.org/10.1038/nsmb.3113

Tang GQ, Patel SS (2006) T7 RNA polymerase-induced bending of promoter DNA is coupled to DNA opening. Biochemistry 45(15):4936–4946. https://doi.org/10.1021/bi0522910

Thommes P, Kubota Y, Takisawa H, Blow JJ (1997) The RLF-M component of the replication licensing system forms complexes containing all six MCM/P1 polypeptides. EMBO J 16(11):3312–3319. https://doi.org/10.1093/emboj/16.11.3312

Ticau S, Friedman LJ, Ivica NA, Gelles J, Bell SP (2015) Single-molecule studies of origin licensing reveal mechanisms ensuring bidirectional helicase loading. Cell 161(3):513–525. https://doi.org/10.1016/j.cell.2015.03.012

Traver S, Coulombe P, Peiffer I, Hutchins JR, Kitzmann M, Latreille D, Mechali M (2015) MCM9 is required for mammalian DNA mismatch repair. Mol Cell 59(5):831–839. https://doi.org/10.1016/j.molcel.2015.07.010

Tye BK (1999a) MCM proteins in DNA replication. Annu Rev Biochem 68:649–686. https://doi.org/10.1146/annurev.biochem.68.1.649

Tye BK (1999b) Minichromosome maintenance as a genetic assay for defects in DNA replication. Methods 18(3):329–334. https://doi.org/10.1006/meth.1999.0793

Yardimci H, Loveland AB, Habuchi S, van Oijen AM, Walter JC (2010) Uncoupling of sister replisomes during eukaryotic DNA replication. Mol Cell 40(5):834–840. https://doi.org/10.1016/j.molcel.2010.11.027

Yeeles JT, Deegan TD, Janska A, Early A, Diffley JF (2015) Regulated eukaryotic DNA replication origin firing with purified proteins. Nature. https://doi.org/10.1038/nature14285

Yonath A (2010) Polar bears, antibiotics, and the evolving ribosome (Nobel lecture). Angew Chem 49(26):4341–4354. https://doi.org/10.1002/anie.201001297

Yuan Z, Bai L, Sun J, Georgescu R, Liu J, O'Donnell ME, Li H (2016) Structure of the eukaryotic replicative CMG helicase suggests a pumpjack motion for translocation. Nat Struct Mol Biol 23(3):217–224. https://doi.org/10.1038/nsmb.3170